

Flickering of the jet-ejecting symbiotic star MWC 560

R. K. Zamanov^{1,*}, S. Boeva¹, K. A. Stoyanov¹, G. Latev¹, B. Spassov¹, A. Kurtenkov¹, and G. Nikolov¹

Institute of Astronomy and National Astronomical Observatory, Bulgarian Academy of Sciences, Tsarigradsko Shose 72, BG-1784 Sofia, Bulgaria

Received 2019 December 3, accepted 2020 March 31

Key words accretion, accretion discs – (stars:) novae, cataclysmic variables – binaries: symbiotic – stars: individual: MWC 560

We analyse optical photometric data of short term variability (flickering) of the accreting white dwarf in the jet-ejecting symbiotic star MWC 560. The observations are obtained in 17 nights during the period November 2011 - October 2019. The colour-magnitude diagram shows that the hot component of the system becomes redder as it gets brighter. For the flickering source we find that it has colour $0.14 < B - V < 0.40$, temperature in the range $6300 < T_{fl} < 11000$ K, and radius $1.2 < R_{fl} < 18 R_{\odot}$. We find a strong correlation (correlation coefficient 0.76, significance < 0.001) between B band magnitude and the average radius of the flickering source – as the brightness of the system increases the size of the flickering source also increases. The estimated temperature is similar to that of the bright spot of cataclysmic variables. In 2019 the flickering is missing, and the B-V colour of the hot component becomes bluer.

Copyright line will be provided by the publisher

1 Introduction

The symbiotic stars are wide binaries with long orbital periods (from 100 days to 100 years) in which material is transferred from an evolved red giant star to a white dwarf or a neutron star (Mikołajewska 2012). The symbiotic star MWC 560 (V694 Mon) was identified as an emission line object at the Mount Wilson observatory spectroscopic surveys (Merrill & Burwell 1943). The spectroscopic observations of MWC 560 in 1984 showed that it is an extraordinary symbiotic star with absorption extending out to -3000 km s^{-1} at H β and higher members of the Balmer series (Bond et al. 1984). In early 1990 the outflow velocities reached $6000 - 7000 \text{ km s}^{-1}$ (Tomov et al. 1990; Szkody, Mateo & Schmeer 1990). Tomov et al. (1990) proposed that the observed absorptions are caused by a collimated outflow along the line of sight – a low-energy analog of the jets of the microquasar SS 433. The outflow may be a highly-collimated baryon-loaded jet (Schmid et al. 2001) or a wind from the polar regions (Lucy, Knigge & Sokolowski 2018). MWC 560 is considered to be a non-relativistic analog of the quasars not only because of its jets, but also to the resemblance of its emission lines to that of the low-redshift quasars (Zamanov & Marziani 2002) and the absorption lines to that of the broad absorption lines quasars (Lucy et al. 2018). The orbital period of the binary is thought to be $P_{orb} = 1931 \pm 162 \text{ d}$ (Gromadzki et al. 2007) although recently Munari et al. (2016) supposed that it could be considerably shorter, $P_{orb} \approx 330.8 \text{ d}$.

Systematic searches for flickering variability in symbiotic stars and related objects (Dobrzycka, Kenyon & Milone

1996; Sokolowski, Bildsten & Ho 2001; Gromadzki et al. 2006; Angeloni et al. 2013) have shown that optical flickering is a rarely detectable phenomenon in symbiotic stars. Among more than 200 symbiotic stars known, only in 11 objects flickering activity is visible. A flickering variability of MWC 560 of up to 0.2 mag on timescale of a few minutes was first reported by Bond et al. (1984). The amplitude is in the range 0.1 – 0.7 mag and the detected quasi-periods are from 11 to 160 min (Tomov et al. 1996). The intra-night variability was a persistent feature till 2018, when the variability on time-scale of minutes became undetectable (Goranskij et al. 2018).

Here, we report quasi-simultaneous observations of the flickering variability of the jet-ejecting symbiotic star MWC 560 (most of them in the two optical bands – B and V) and analyze the colour changes, temperature and radius of the flickering source and their response to the brightness variations.

2 Observations and data analysis

The observations were performed with four telescopes equipped with CCD cameras:

- the 2.0 m telescope of the National Astronomical Observatory (NAO) Rozhen, Bulgaria (Bonev & Dimitrov 2010)
- the 50/70 cm Schmidt telescope of NAO Rozhen
- the 60 cm telescope of NAO Rozhen
- the 60 cm telescope of the Belogradchik Observatory, Bulgaria (Strigachev & Bachev 2011)

The data reduction was done with IRAF (Tody 1993) following standard recipes for processing of CCD images and

* Corresponding author: rkz@astro.bas.bg

aperture photometry. A few comparison stars from the list of Henden & Munari (2006) and APASS DR9 have been used. The typical photometric errors are 0.007 mag in U-band, 0.005 mag in B-band, and 0.004 mag in V-band.

Three examples of our data are given on Fig. 1. On the left panel (20110210) are plotted UBVR data. The amplitude in U-band is 0.47 mag, in B-band - 0.34 mag, in V-band - 0.32 mag, in R-band - 0.23 mag, in I-band - 0.07 mag. The amplitude of the flickering is decreasing to longer wavelengths, mainly due to the increasing contribution of the red giant, which is the dominating source in infrared bands. In the middle panel (20170222), the light curves of MWC 560 in B- and V-bands are plotted together with the calculated B-V colour. The right panel are UBVR data obtained on 20191025 when the flickering is missing. If it exists at all its amplitude in UBVR is < 0.02 mag.

We have 17 nights with simultaneous observations in B and V bands during the period July 2008 - October 2019. The $B - V$ colour is calculated for 2307 points in total. During our observations the brightness of MWC 560 was:

$$9.20 \leq B \leq 11.92,$$

$$8.60 \leq V \leq 11.33,$$

$$0.31 \leq B - V \leq 0.67,$$

with mean $B = 10.28$, mean $V = 9.81$, mean $B - V = 0.47$. When the flickering exists, its peak-to-peak amplitude in B band is in the range 0.13 - 0.39 mag.

The journal of observations is given in Table 1. In Table 2 are given the number of data points over which B-V colour is calculated, average, minimum and maximum magnitude in B- and V-bands.

3 Parameters of the system

GAIA DR2 (Gaia Collaboration et al. 2018) gives for MWC560 parallax 0.3534 ± 0.1659 , which corresponds to a distance $d=2830$ pc. Schmid et al. (2001) derived distance 2.5 ± 0.7 kpc, which agrees with the GAIA value.

Schmid et al. (2001) estimated interstellar extinction $E(B-V)=0.15$ mag from 2200 Å feature and for the mass donor spectral type M5.5 III. Slightly different values are given earlier by Zhekov et al. (1996) - M4.5 III and $E(B-V)=0.23$ mag. Most likely the extinction is in the range $0.1 \leq E(B - V) \leq 0.2$ in the light of the NaD absorption and dust maps (Lucy et al. 2020). Houdashelt, Wyse & Gilmore (2001) give for M5.5 III giant colours $B-V=1.55$ and $V-I=2.7$.

For the red giant, Zhekov et al. (1996) estimated $m_B \sim 14$ mag, which is in agreement with the long term light curve of MWC 560 (Doroshenko, Goranskij & Efimov 1993). With the above colour and extinction, this give for the red giant $m_V \sim 12.30$ mag. Using J and K-band data from 2MASS All Sky Catalog ($J=6.452$, $K=5.069$) and the extinction law from Savage & Mathis (1979), we obtain $A_J = 0.13$ and $A_K = 0.06$. Koornneef (1983) gives an intrinsic colours $V-K = 6.7$ and $V-J = 5.43$ for an M5.5 III star. Us-

ing these parameters, we derive $m_V = 12.23$ and $m_V = 12.19$ using J and K-band respectively.

Hereafter, we assume for the red giant component of MWC 560, $m_V \approx 12.25$ and $m_B \approx 13.94$. These magnitudes are used in Sect. 4 to estimate the colours of the hot component.

4 Variability in B and V bands

In Fig.2 we plot B versus V band magnitude. In the left panel (Fig. 2a) are the observed magnitudes of MWC 560. In the right panel (Fig. 2b) are the de-reddened magnitudes of the hot component (e.g. the red giant contribution is subtracted using the magnitudes given in Sect. 3).

In Fig.3 we plot colour-magnitude diagrams. The colour-magnitude diagram is quite different from that of the cataclysmic variable AE Aqr (see Fig.3 in Zamanov et al. 2017) but it is similar to that of the recurrent nova RS Oph (see Fig. 3,4,5 in Zamanov et al. 2018). In the case of AE Aqr all the data occupy a well defined strip. Here such a strip is not visible, although the observations from each night are placed on a specific position on the diagram. This indicates that the flickering behaviour of MWC 560 has a similar mechanism to that of RS Oph, but different than that of AE Aqr.

In Fig.4 we plot the calculated mean values for each night (one night - one point). The error bars correspond to the standard deviation of the run. The left panel is the observed, the right panel is the hot component (red giant contribution subtracted). On Fig.4a, it can be seen that the colour of the system is in the range $0.31 \leq B - V \leq 0.67$, without clear tendency to become redder or bluer when the brightness changes.

However, there is a correlation between the mean colour and magnitude of the hot component. When we use the 15 points, when the flickering exists we calculate Pearson correlation coefficient 0.91, Spearman's (rho) rank correlation 0.88, the statistical significance p -value = 5.9×10^{-5} . This indicates that the hot component becomes redder as it gets brighter.

When we use all 17 points including the two nights without flickering this correlation weakens: Pearson correlation coefficient 0.58, Spearman's (rho) rank correlation 0.45 p -value = 0.07. This indicates that the missing flickering is connected with violation of colour - brightness relation of the accretion disc and/or probably changes in its structure/geometry.

5 Flickering light source

Bruch (1992) proposed that the light curve of a white dwarf with flickering can be separated into two parts - constant light and variable (flickering) source. Following his recipe, we calculate the flux of the flickering light source as $F_{fl} = F_{av} - F_{min}$, where F_{av} is the average flux during the run

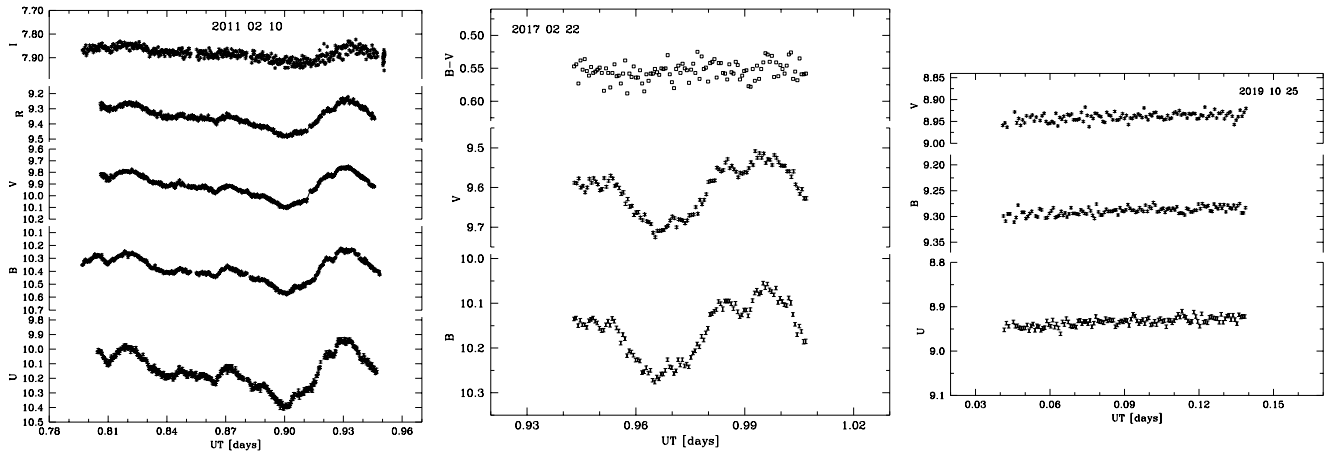


Fig. 1 Examples of the short term variability of MWC 560. The label in each panel indicate the date of observations in format YYYYMMDD. The left panel is 20110210 – UBVR data (the flickering is visible even in I band, its amplitude is decreasing to the red bands). The middle panel is 20170222 – the light curves in B and V bands together with the calculated B-V colour. The right panel is 20191025 - UB data, the flickering is missing.

Table 1 Journal of observations. In the table are given the date of observations, the telescope, the filter, UT start and end of the run, detection/non-detection of flickering.

Date yyyymmdd	telescope	bands	UT start - UT-end	detection
20091114	2.0 Roz	U	23:59 – 01:27	yes
	50/70 Sch	B	00:21 – 01:32	yes
	60 Bel	V	00:22 – 01:27	yes
	60 Roz	R	00:14 – 01:34	yes
20100111	2.0 Roz	U, V	23:31 – 01:04	yes
	50/70 Sch	B	23:28 – 01:10	yes
	60 Roz	R, I	23:13 – 01:01	yes
20100315	60 Roz	V, I	18:00 – 19:15	yes
20100317	60 Roz	V, I	18:08 – 19:14	yes
20101229	2.0 Roz	U	22:55 – 01:28	yes
	60 Bel	V, R	22:10 – 01:30	yes
	60 Roz	B, I	21:53 – 01:31	yes
20110210	2.0 Roz	U	19:18 – 22:43	yes
	60 Roz	B, I	19:07 – 22:45	yes
	60 Bel	V, R	19:20 – 22:41	yes
20110211	60 Roz	U, B	19:35 – 22:59	yes
	60 Bel	V, R, I	19:34 – 23:01	yes
20110212	60 Roz	U, B, V, R, I	20:25 – 22:47	yes
20120321	60 Bel	B, V, R	18:27 – 20:20	yes
20120323	60 Bel	B, V, R, I	18:06 – 20:15	yes
20130303	60 Bel	B, V, R, I	19:35 – 21:10	yes
20130305	60 Bel	B, V, R, I	18:37 – 20:31	yes
20131129	60 Roz	B, V, R, I	00:26 – 03:31	yes
20151118	60 Bel	B, V, R, I	02:10 – 04:19	yes
20160402	60 Bel	B, V	18:12 – 19:25	yes
20160405	50/70 Sch	B	17:40 – 19:11	yes
20170222	60 Bel	B, V	22:37 – 00:09	yes
20180124	50/70 Sch	B, V, R, I	22:18 – 22:50	yes
20191022	50/70 Sch	B, V	00:17 – 03:49	no
20191025	50/70 Sch	U, B, V	00:59 – 03:19	no
20200201	50/70 Sch	B	19:50 – 21:15	no

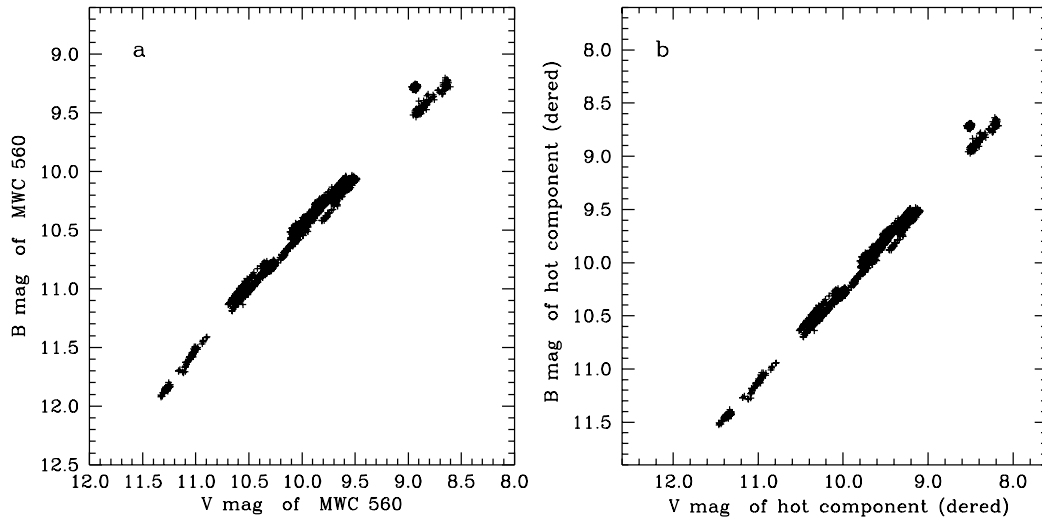


Fig. 2 B versus V band magnitude: a) observed, b) calculated for the hot component.

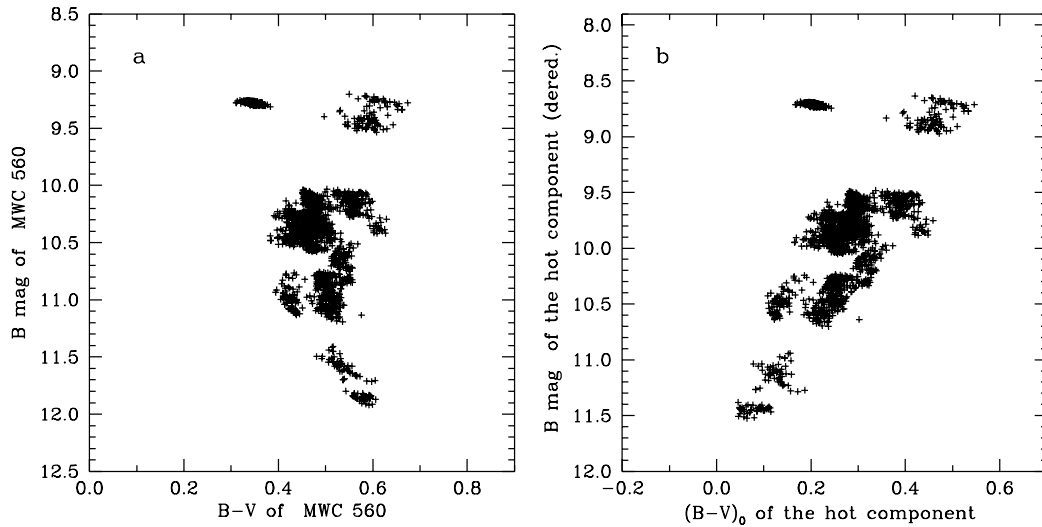


Fig. 3 Colour magnitude diagram: a) observed, b) calculated for the hot component.

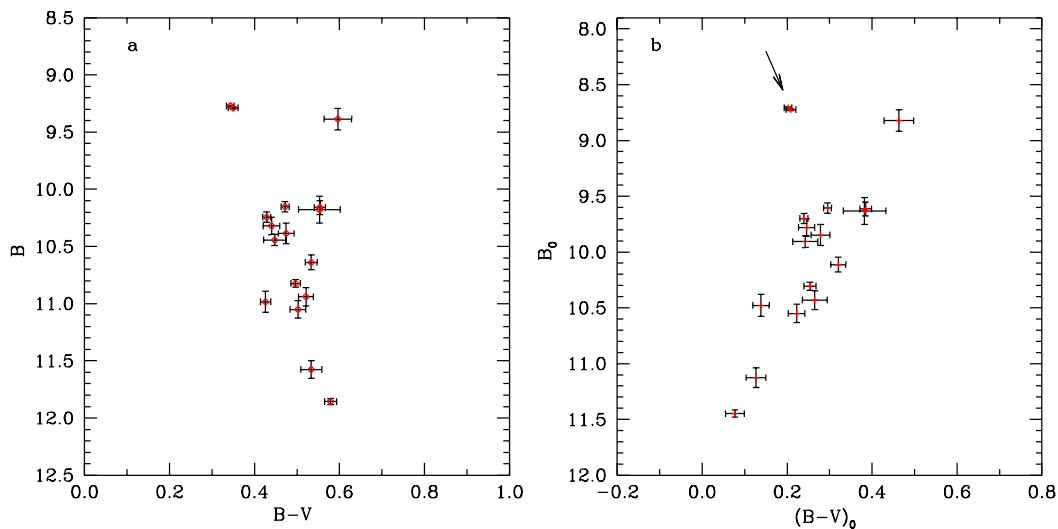


Fig. 4 Mean colour magnitude diagram, each point represent one run: a) observed, b) calculated for the hot component, the arrow indicates the two nights without detectable flickering.

Table 2 Data used to calculate the B-V colour of MWC 560. In the Table are given the date, N_{pts} (the number of data points over which B-V colour is calculated), average, minimum and maximum magnitudes in B and V bands.

date YYYYMMDD	N_{pts}	mean(B) [mag]	min(B) [mag]	max(B) [mag]	mean(V) [mag]	min(V) [mag]	max(V) [mag]
20091114	39	11.8557	11.799	11.921	11.2766	11.240	11.329
20100111	52	11.5749	11.410	11.715	11.0412	10.894	11.163
20101229	360	10.1520	10.040	10.245	9.6801	9.587	9.778
20110210	477	10.3856	10.224	10.580	9.9110	9.747	10.108
20110211	186	10.4426	10.331	10.568	9.9949	9.899	10.116
20110212	143	10.3205	10.205	10.460	9.8805	9.776	10.018
20120321	70	10.6389	10.496	10.752	10.1055	9.9440	10.205
20120323	93	10.9392	10.776	11.079	10.4181	10.227	10.577
20130303	100	10.8227	10.755	10.888	10.3261	10.247	10.394
20130305	79	11.0507	10.880	11.191	10.5484	10.385	10.662
20131129	75	10.9839	10.764	11.134	10.5579	10.331	10.696
20151118	87	10.1774	10.032	10.420	9.6246	9.481	9.813
20160402	88	9.3861	9.202	9.535	8.7897	8.605	8.953
20170222	110	10.1601	10.055	10.276	9.6060	9.508	9.725
20180124	27	10.2431	10.134	10.299	9.8144	9.716	9.868
20191022	207	9.2703	9.254	9.293	8.9272	8.909	8.950
20191025	114	9.2885	9.273	9.311	8.9387	8.917	8.967

and F_{\min} is the minimum flux during the run (corrected for the typical error of the observations). An expansion of the method is proposed by Nelson et al. (2011). They suggest to use the $F_{\text{fl}2} = F_{\max} - F_{\min}$, where F_{\max} is the maximum flux during the run. In fact, the method of Bruch (1992) evaluates the average brightness of the flickering source, while that of Nelson et al. (2011) – its maximal brightness. $F_{\text{fl}1}$ and $F_{\text{fl}2}$ have been calculated for each band, using the values given in Table 2 and the calibration for a zero magnitude star $F_0(B) = 6.293 \times 10^{-9} \text{ erg cm}^{-2} \text{ s}^{-1} \text{ \AA}^{-1}$, $\lambda_{eff}(B) = 4378.12 \text{ \AA}$, $F_0(V) = 3.575 \times 10^{-9} \text{ erg cm}^{-2} \text{ s}^{-1} \text{ \AA}^{-1}$ and $\lambda_{eff}(V) = 5466.11 \text{ \AA}$ as given in Spanish virtual observatory Filter Profile Service (Rodrigo et al. 2018, see also Bessell 1979).

It is worth noting that while the calculated colours of the hot component depend on the assumed red giant brightness, the parameters of the flickering source are independent on the red giant parameters.

Using method of Bruch (1992), we find that in B band the flickering light source contributes about 12% of the average flux of the system, with $0.06 \leq F_{\text{fl}1}/F_{\text{av}} \leq 0.20$. In V band its average contribution is 11%, with $0.05 \leq F_{\text{fl}1}/F_{\text{av}} \leq 0.17$.

Using method of Nelson et al. (2011), we find that in B band the flickering light source contributes about 22% of the maximal flux of the system, with $0.11 \leq F_{\text{fl}2}/F_{\max} \leq 0.30$. In V band its is about 21%, with $0.08 \leq F_{\text{fl}2}/F_{\max} \leq 0.29$.

From the amplitude - flux relation (rms-flux relation) e.g. Scaringi et al. (2015), we expect that the luminosity of the flickering source will increase as the brightness increases. However, it is not a priori clear which parameter – temperature or radius (or both), increases.

In Table 3 are given the dereddened colour of the flickering source $(B - V)_{01}$ and $(B - V)_{02}$, T_1 and T_2 - temperature

of the flickering source, R_1 and R_2 - radius the flickering source.

In the calculations we assume that the flickering source is continuum dominated. In principle, it is possible that the flickering involves both continuum and lines. However, the search for rapid spectral variability related to the flickering in MWC 560 shows that there are no changes higher than a few per cent level in the optical lines in spite of 0.35 mag flickering in B band (Tomov et al. 1995). Our simultaneous 5-colour photometry shows that the flickering source is well approximated with black body in the UBVRi bands (Zamanov et al. 2011b). The observations of the near-UV flickering, show that near-UV spectral morphology remained constant so the near-UV flickering must have originate in a variable continuum (Lucy et al. 2020). Bearing in mind the above, as well the discussion in Sect. 6.2 of Sokoloski et al. (2001) about the difficulty of producing rapid variability from the nebular emission, we adopt that the flickering of MWC 560 is continuum dominated and reflects the physical origin of the variations in the accretion disc around the white dwarf.

5.1 B-V colour and temperature of the flickering source

The calculated de-reddened colours of the flickering light source are given in Table 3, where $(B - V)_{01}$ is calculated using F_{av} and F_{\min} , while $(B - V)_{02}$ is calculated using F_{\max} and F_{\min} . Typical error is ± 0.05 mag.

In Fig.5 we plot $(B - V)_{02}$ versus $(B - V)_{01}$. The solid line represents $(B - V)_{02} = (B - V)_{01}$. To check for a systematic shift between the two methods we performed linear least-squares approximation in one-dimension ($y = a + bx$), when both x and y data have errors. We obtain $a = 0.01 \pm 0.02$ and $b = 0.95 \pm 0.07$. A Kolmogorov-Smirnov test gives

Kolmogorov-Smirnov statistic 0.07 and significance level 0.99. It means that both methods give similar results and there is not a systematic shift. The average difference between them is ≈ 0.07 mag, which is comparable with the accuracy of our estimations. In Fig. 6, we plot $(B - V)_0$ versus the average B band magnitude. We do not detect a statistically significant correlation between the colour of the flickering source and the brightness of the system.

We calculate the temperature of the flickering source using its dereddened colours and the colours of the black body (Straizys, Sudzius & Kuriliene 1976). T_1 is calculated using $(B - V)_{01}$, and T_2 is calculated using $(B - V)_{02}$. The two methods give similar results for the temperature of the flickering source as well as for $(B - V)_0$. The average values are $T_1 = 8244 \pm 1180$ and $T_2 = 8241 \pm 1290$.

5.2 Radius and luminosity of the flickering source

The radius of the flickering source is calculated using the derived temperature (Sect. 5.1), the B-band magnitude and assuming that it is spherically symmetric. We obtain $1.2 < R_1 < 13.6 R_\odot$ and $1.3 < R_2 < 18.7 R_\odot$. In Fig. 7 we plot R_1 and R_2 versus the average B band magnitude. It is seen that radius of the flickering source increases when the brightness of the system increases.

The luminosity of the flickering source is calculated using the derived temperature and the radius given in Table 3: $L_1 = 4\pi R_1^2 \sigma T_1^4$, where σ is the Stefan-Boltzmann constant. We obtain $10.4 L_\odot < L_1 < 260 L_\odot$, and $22 L_\odot < L_2 < 600 L_\odot$.

We found a strong correlation between the average B band magnitude and R_1 with Pearson correlation coefficient 0.765, Spearman's (rho) rank correlation 0.761, significance p -value = 9.9×10^{-4} . The correlation between B and R_2 is weaker. There are also strong correlations between B and L_1 – Pearson 0.785, Spearman 0.782, p -value = 5.7×10^{-4} , as well as between B and L_2 – Pearson 0.79, Spearman's 0.80, p -value = 3.0×10^{-4} .

6 Discussion

During the last decades, MWC 560 underwent three optical brightenings - 1990, 2010-2011 and 2016. Multiwavelength observations (including optical, ultraviolet, X-ray and radio data) in the last years as well as a model accounting for the similarities and the differences between the brightening events is presented by Lucy et al. (2020). The observations of the intranight variability during the 1990 outburst are presented and analysed in Tomov et al. (1996) and Zamanov et al. (2011a). The present data set covers the period 2009 – 2019. The long term light curve (Doroshenko et al. 1993; Leibowitz & Formiggini 2015) indicates that during our observations MWC 560 was on average 3-4 times brighter in the optical bands than before 1989.

Random fluctuations of the brightness are observed throughout diverse classes of objects that accrete material

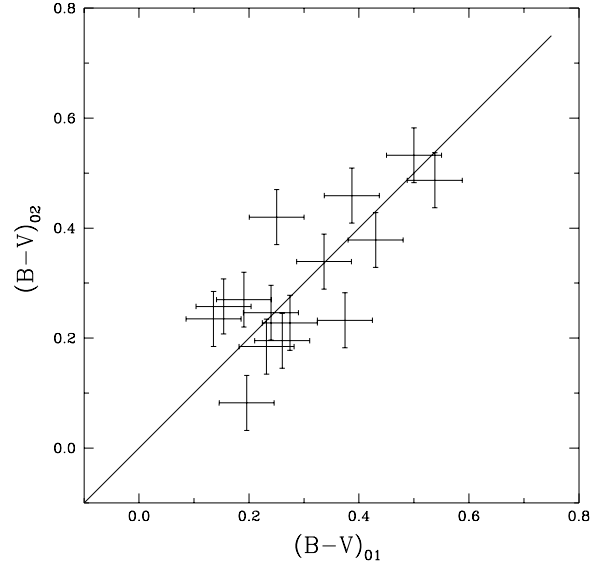


Fig. 5 $(B - V)_{02}$ versus $(B - V)_{01}$ – there is no systematic shift between the two methods. See Sect. 5.1 for details.

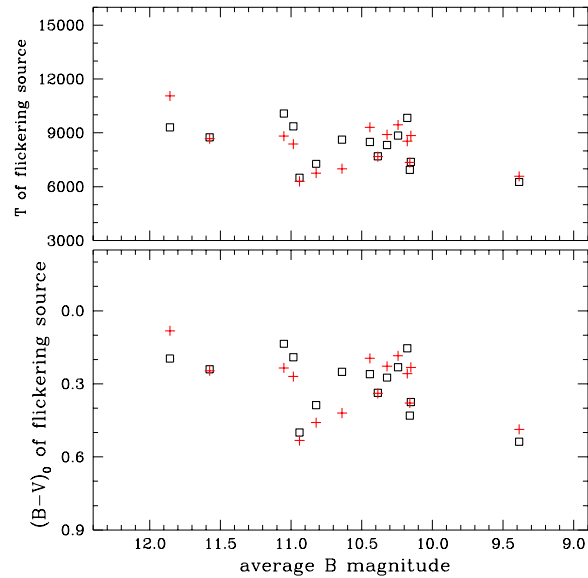


Fig. 6 Temperature and $(B - V)_0$ colour of the flickering source versus the average B magnitude. The squares represent values calculated by method of Bruch (1992), the plus signs – derived following Nelson et al. (2011).

onto a compact object (white dwarf, neutron star or black hole) – cataclysmic variables, X-ray binaries, Active Galactic Nuclei. Photoelectric observations identified the flickering as a common characteristic of the accreting white dwarfs in cataclysmic variables (e.g. Mumford 1966, Henize 1949, Robinson 1973). The flickering appears as stochastic light variations on time-scales of about 10 minutes with amplitude from a few $\times 0.01$ mag to more than one magnitude. Three different places are considered as source of flickering from accreting white dwarfs – the accretion disc itself,

Table 3 The calculated parameters of the flickering source of MWC 560. $(B - V)_{01}$, T_1 and R_1 are dereddened colour, temperature and radius of the flickering source calculated following Bruch (1992), $(B - V)_{02}$, T_2 and R_2 – following Nelson et al. (2011), see Sect. 5 for details.

date YYYYMMDD	$(B - V)_{01}$	T_1 [K]	R_1 [R_\odot]	$(B - V)_{02}$	T_2 [K]	R_2 [R_\odot]
20091114	0.1958	9302	1.24	0.0821	11053	1.28
20100111	0.2400	8750	2.27	0.2461	8674	3.55
20101229	0.3744	7380	5.14	0.2323	8846	5.38
20110210	0.3365	7696	5.94	0.3391	7674	8.41
20110211	0.2604	8495	3.85	0.1952	9310	4.57
20110212	0.2743	8321	4.46	0.2277	8904	5.43
20120321	0.2503	8621	3.25	0.4199	7001	7.92
20120323	0.5001	6499	5.88	0.5325	6297	9.76
20130303	0.3870	7275	3.29	0.4591	6756	5.67
20130305	0.1355	10082	2.24	0.2348	8815	4.42
20131129	0.1907	9366	2.71	0.2699	8376	5.55
20151118	0.1537	9829	4.50	0.2575	8531	7.65
20160402	0.5379	6263	13.63	0.4870	6581	18.74
20170222	0.4304	6935	6.57	0.3784	7347	8.13
20180124	0.2319	8851	2.64	0.1845	9444	4.13

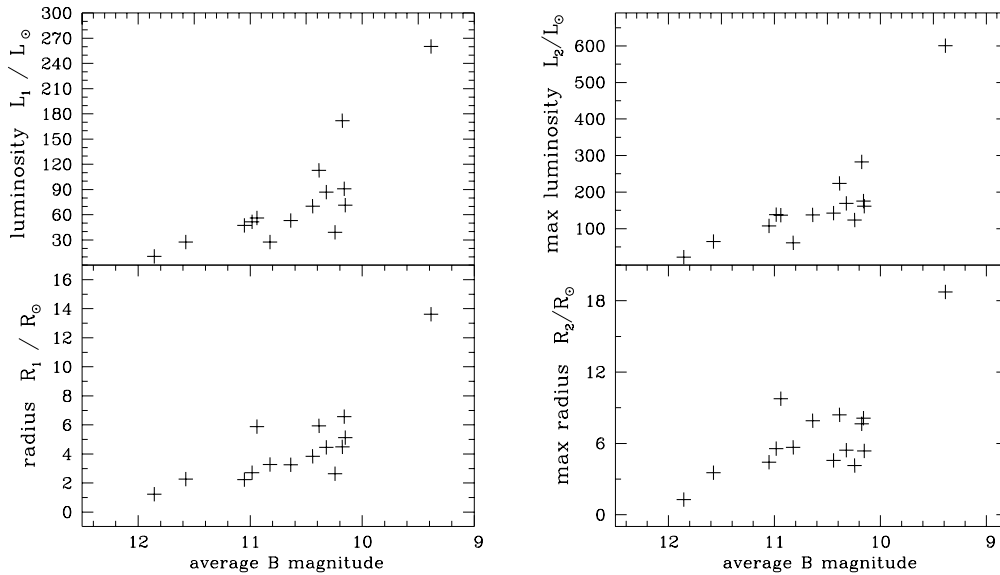


Fig. 7 Radius and luminosity of the flickering source of MWC 560 versus the average B band magnitude. The left panels are average L_1 and R_1 , the right are the maximum L_2 and R_2 (see Sect. 5).

its outer edge (bright spot), and its inner edge (boundary layer).

6.1 Bright spot

The temperature and the size of the bright spot are derived for a few cataclysmic variables. For OY Car, Wood et al (1989) calculated temperature in the range 8600 – 15000 K; Zhang & Robinson (1987) for U Gem - $T = 11600 \pm 500$

K; Robinson, Nather & Patterson (1978) give $T = 16000$ K for the bright spot in WZ Sge. For IP Peg three estimates exist: Marsh (1988) – $T = 12000 \pm 1000$ K, Ribeiro et al. (2007) – 6000-10000 K, Copperwheat et al. (2010) – 7000 - 13000 K. The temperature of the optical flickering source of MWC 560 is in the range $6200 < T_{fl} < 10100$ K (see Sect.4.1), which is similar to the temperature of the bright spot of cataclysmic variable stars.

The bright spot is produced by the impact of the stream on the outer parts of the accretion disc. In case of Roche-lobe overflow this stream is coming from the inner Lagrangian point L_1 . If the red giant in MWC 560 does not fill its Roche lobe, the white dwarf accretes material from its wind. In this case accretion cone and accretion wake will be formed, e.g. Fig. 4 of Ahmad, Chapman & Kondo (1983). The stream formed in the accretion wake should be similar to that formed from Roche-lobe overflow. The luminosity of the bright spot is approximately (Shu 1976; Elsworth & James 1982):

$$L_{bs} \approx \frac{1}{2} V_{\perp}^2 \dot{M}_{acc}, \quad (1)$$

where \dot{M}_{acc} is the mass accretion rate and V_{\perp} is the inward component of the stream's velocity at the impact with the disc. Eq. 1 indicates that when the mass accretion rate increases, the luminosity of the spot also must increase. In addition, our results (Sect. 5.2) indicate that when the mass accretion rate increases the radius of the bright spot (if it is the source of flickering) also increases, while its temperature remains almost constant.

6.2 Temperature in the accretion disc

The broad-band variability is often attributed to **(i)** inward propagating fluctuations driven by stochastic variability in the angular momentum transport mechanism (Lyubarskii 1997); **(ii)** turbulence, vortexes in the disc (e.g. Dobrotka et al. 2010; Kurbatov & Bisikalo 2017); **(iii)** spiral structures in the disc (e.g. Baptista & Bortoletto 2008). The timescales of changes of the overall structure of the accretion disc are longer compared to the local fluctuating processes in the flow that can generate the flickering. In this way the dynamical time scale variability of the flickering light source do not change the overall structure of the accretion disc. Considering the entire disc structure, the temperature in the disc can be approximated with the radial temperature profile of a steady-state accretion disc (e.g. Frank, King & Raine 2002):

$$T_{eff}^4 = \frac{3G\dot{M}_{acc}M_{wd}}{8\pi\sigma R^3} \left[1 - \left(\frac{R_{wd}}{R} \right)^{1/2} \right], \quad (2)$$

R is the radial distance from the white dwarf. We assume $M_{wd} = 0.9 M_{\odot}$ and $R_{wd} = 6 \times 10^8$ cm (Zamanov, Gomboc, & Latev 2011; Lucy et al. 2020) and mass accretion rate of about $5 \times 10^{-7} M_{\odot} \text{ yr}^{-1}$ (Schmid et al. 2001).

Using the parameters for MWC 560, a temperature $6300 \leq T_{fl} \leq 10000$ K (the temperature of the flickering light source as given in Table 3) should be achieved at a distance $R \approx 1.2 - 2.5 R_{\odot}$ from the white dwarf. If the accretion disc itself is the place for the origin of the flickering of MWC 560, then it comes at distance $R \sim 2 R_{\odot}$ from the white dwarf.

6.3 Boundary layer

The boundary layer between the white dwarf and the inner edge of the accretion disc should have temperature $\geq 10^5$ K

(e.g. Mukai 2017). The derived temperature of the flickering source is considerably lower than that expected from the boundary layer. If the boundary layer is optically thick, in this case the radius of the flickering source measured in the optical bands (Fig. 7) could represent the radius up to which the emission generated from the boundary layer is reprocessed by the inner parts of the accretion disc and the accretion disc corona.

6.4 Disappearance of the flickering

The first indication that flickering of symbiotic stars disappears sometimes was found for the recurrent nova T CrB (Bianchini & Middleditch 1976). In CH Cyg the flickering was missing for more than 3 years (Stoyanov et al. 2018). In RS Oph the flickering disappeared after the nova outburst and re-appeared 241 days later (Worters et al. 2007). In MWC 560 the flickering was visible in all observations obtained between 1984 and May 2018 (Tomov et al. 1996, Zamanov et al. 2011a,b; Lucy et al. 2020). It disappeared in October 2018 (Goranskij et al. 2018) and is not visible in our observations obtained in October 2019 and February 2020. What can be the reason for disappearance of the flickering :

1. If the source of the flickering is bright spot than it means that for some reason $V_{\perp} \approx 0$ (see Eq. 1). In other words at the impact point, the stream has velocity approximately equal to the velocity of the outer disc edge.
2. If the source of the flickering is the accretion disc, the disappearance means that the stochastic fluctuations disappear and the disc becomes stable (non-fluctuating).
3. Goranskij et al. (2018) proposed that a common envelope is formed due to the transit of the system to a dynamical mode of accretion with an increased rate. The accretion matter filling the Roche lobe of the compact companion blocked the jets and overlapped the direct visibility of the companion, so flickering was deleted.

In MWC 560 at the disappearance of the flickering the hot component becomes bluer, but its brightness in B band remain high (see Fig. 4b, where the arrow indicates the observations without flickering). This could be an indication that the accretion disc becomes smaller and/or hotter.

In X-rays MWC 560 is β/δ type, i.e. with two X-ray thermal components – soft and hard (Luna et al. 2013). The soft emission is most likely produced in a colliding-wind region, and the hard emission is most likely produced in boundary layer between accretion disc and white dwarf. The changes in the X-ray emission can give us clues why the flickering disappeared.

7 Conclusions

We report quasi-simultaneous observations of the flickering variability of the jet-ejecting symbiotic star MWC 560 in 17 nights during the period November 2011 - October 2019.

The colour-magnitude diagram, B versus B-V, shows that when the flickering exists, the hot component of the system becomes redder as it gets brighter.

For the flickering source we find that it has colour in the range $0.14 < B - V < 0.40$, temperature in the range 6300 – 11000 K, and radius in the range 1.2 – 18 R_{\odot} . The estimated temperature is similar to that of the bright spot of cataclysmic variables. We do not find a correlation between the temperature of the flickering and the brightness. However, we do find strong correlations (1) between B band magnitude and the average radius of the flickering source – as the brightness of the system increases the size of the flickering source also increases; (2) between B band magnitude and the luminosity of the flickering source – as the brightness of the system increases the luminosity of the flickering source also increases. When the flickering disappeared in 2019, the B-V colour of the hot component becomes bluer and its brightness in UBV remains high.

The behaviour of the hot component and flickering source in MWC 560 should provide useful input for theoretical modeling of accretion in symbiotic type binaries.

Acknowledgements: We dedicate this paper to the memory of Prof Toma Tomov (1953 - 2019), who initiated the observations of MWC 560 at Rozhen Observatory. This work was supported by the grant KP-6-H28/2 "Binary stars with compact object" (Bulgarian National Science Fund).

References

- Ahmad, I. A., Chapman, R. D., Kondo, Y. 1983, *A&A*, 126, L5
 Angeloni, R., Di Mille, F., Lopes, C. E. F., Masetti, N. 2013, *IAUS*, 179, *IAUS*..290
 Baptista, R. & Bortoletto, A. 2008, *ApJ*, 676, 1240
 Bessell, M. S. 1979, *PASP*, 91, 589
 Bianchini, A., Middleditch J. 1976, *IBVS*, 1151, 1
 Bond, H. E., Pier, J., Pilachowski, C., Slovak, M., Szkody, P. 1984, *BAAS*, 16, 516
 Bonev, T. & Dimitrov D. 2010, *BlgAJ*, 13, 153
 Bruch, A. 1992, *A&A*, 266, 237
 Copperwheat, C. M., Marsh, T. R., Dhillon, V. S., Littlefair, S. P., Hickman, R., Gänsicke, B. T., Southworth, J. 2010, *MNRAS*, 402, 1824
 Dobrotka, A., Hric, L., Casares, J., Shahbaz, T., Martínez-Pais, I. G., Muñoz-Darias, T. 2010, *MNRAS*, 402, 2567
 Dobrzycka, D., Kenyon, S. J., Milone, A. A. E. 1996, *AJ*, 111, 414
 Doroshenko, V. T., Goranskij, V. P., Efimov, Y. S. 1993, *IBVS*, 3824, 1
 Elsworth, Y. P. & James J. F. 1982 *MNRAS*, 198, 889
 Frank, J., King, A., Raine, D. J. 2002, *Accretion Power in Astrophysics: Third Edition*, CUP
 Gaia Collaboration, Brown, A. G. A., Vallenari, A., et al. 2018, *A&A*, 616, 1
 Goranskij, V. P., Zharova, A. V., Barsukova, E. A., Burenkov, A. N. 2018, *ATel*, 12227, 1
 Gromadzki, M., Mikołajewski, M., Tomov, T., Bellas-Velidis, I., Dapergolas, A., Galan, C. 2006, *AcA*, 56, 97
 Gromadzki, M., Mikołajewska, J., Whitelock, P. A., Marang, F. 2007, *A&A*, 463, 703
 Henden, A., & Munari, U. 2006 *A&A*, 458, 339
 Henize, K. G. 1949, *AJ*, 54, 89
 Houdashelt, M. L., Wyse, R. F. G., Gilmore, G. 2001, *PASP*, 113, 49
 Koornneef, J. 1983, *A&A*, 500, 247
 Kurbatov, E. P. & Bisikalo, D. V. 2017, *ARep*, 61, 475
 Leibowitz, E. M., Formiggini, L. 2015, *AJ*, 150, 52
 Lucy, A. B., Knigge C., Sokoloski J. L. 2018, *MNRAS*, 478, 568
 Lucy, A. B., Sokoloski, J. L., Munari, U. et al. 2020, *MNRAS*, 492, 3107
 Luna, G. J. M., Sokoloski, J. L., Mukai, K., Nelson, T. 2013, *A&A*, 559, A6
 Lyubarskii, Y. E. 1997, *MNRAS*, 292, 679
 Marsh, T. R. 1988, *MNRAS*, 231, 1117
 Merrill, P. W., Burwell, C. G. 1943, *ApJ*, 98, 153
 Mikołajewska, J. 2012, *BaltA*, 21, 5
 Mukai, K. 2017, *PASP*, 129, 062001
 Mumford, G. S. 1966, *ApJ*, 146, 411
 Munari, U. et al. 2016, *NewA*, 49, 43
 Nelson, T., Mukai, K., Orio, M., Luna, G. J. M., Sokoloski, J. L. 2011, *ApJ*, 737, 7
 Robinson, E. L. 1973, *ApJ*, 183, 193
 Robinson, E. L., Nather R. E., Patterson J. 1978, *ApJ*, 219, 168
 Ribeiro, T., Baptista, R., Harlaftis, E. T., Dhillon, V. S., Rutten, R. G. M. 2007, *A&A*, 474, 213
 Rodrigo, C., Solano, E., Bayo, A. 2018, The SVO Filter Profile Service, available at: <http://ivoa.net/documents/Notes/SVOFPS/index.html>
 Savage, B. D., & Mathis, J. S. 1979, *ARA&A*, 17, 73
 Scaringi, S., et al. 2015, *SciA*, 1, e1500686
 Schmid, H. M., Kaufer, A., Camenzind, M., et al. 2001, *A&A*, 377, 206
 Shu, F. H., 1976, *IAU Symposium*, 73, 253
 Sokoloski, J. L., Bildsten, L., Ho, W. C. G. 2001, *MNRAS*, 326, 553
 Stoyanov, K. A., et al. 2018, *BlgAJ*, 28, 42
 Straizys V., Sudzius J., Kuriliene G., 1976, *A&A*, 50, 413
 Strigachev, A. & Bachev R. 2011, *BlgAJ*, 16, 144
 Szkody, P., Mateo, M., Schmeer, P. 1990, *IAUC*, 4987, 1
 Tody, D. 1993, *ASPC*, 173, *ASPC*...52
 Tomov, T., Kolev, D., Georgiev, L., Zamanov, R., Antov, A., Belas, Y. 1990, *Natur*, 346, 637
 Tomov, T., Kolev, D., Munari, U., Sostero, G., Lepardo, A. 1995, *A&A*, 300, 769
 Tomov, T., Kolev, D., Ivanov, M., et al. 1996, *A&AS*, 116, 1
 Wood, J. H., Horne, K., Berriman, G., Wade, R. A. 1989, *ApJ*, 341, 974
 Worters, H. L., Eyres, S. P. S., Bromage, G. E., Osborne, J. P. 2007, *MNRAS*, 379, 1557
 Zamanov, R. K., Tomov, T., Bode, M. F., Mikołajewski, M., Stoyanov, K. A., Stanishev, V. 2011a, *BlgAJ*, 16, 3
 Zamanov, R., Boeva, S., Latev, G., Stoyanov, K., Bode, M. F., Antov, A., Bachev, R. 2011b, *IBVS* 5995, 1
 Zamanov R., Gomboc A., Latev G. 2011, *BlgAJ*, 16, 18
 Zamanov R. K., Latev G. Y., Boeva S., Ibryamov S., Nikolov G. B., Stoyanov K. A. 2017, *AN*, 338, 598
 Zamanov, R. K., Boeva, S., Latev, G. Y., Martí, J., Boneva, D., Spassov, B., Nikolov, Y., Bode, M. F., Tsvetkova, S. V., Stoyanov, K. A. 2018, *MNRAS*, 480, 1363
 Zamanov, R. & Marziani, P. 2002, *ApJL*, 571, L77
 Zhang, E.-H. & Robinson, E. L. 1987, *ApJ*, 321, 813
 Zhekov, S. A., Hunt, L. K., Tomov, T., Gennari, S. 1996, *A&A*, 309, 800